

Pyroelectric AlGaIn/GaN HEMTs for ion-, gas- and polar-liquid sensors

(NICOP Progress Report, 18th month)

Prof. Dr. Oliver AMBACHER (PI), Dr. Vadim LEBEDEV¹

Technical University Ilmenau, Center for Micro- and Nanotechnologies, PO 100565, 98684 Ilmenau, Germany, e-mail: oliver.ambacher@tu-ilmenau.de

Dr. Ute KAISER

University Jena, Institute of Solid State Physics, Max-Wien-Platz 1, 07743 Jena, Germany, e-mail: kaiser@pinet.uni-jena.de

Prof. Dr. L. F. Eastman,

Cornell University, Electrical and Computer Engineering, 425 Phillips Hall, Ithaca, NY 14853-5401, e-mail: lfe@ee.cornell.edu.

Award Number:

N00014-03-1-0301



Center for Micro- and Nanotechnologies
Technical University Ilmenau, Germany

¹ Contact: Dr. V. Lebedev, Technical University Ilmenau, Center for Micro- and Nanotechnologies, PO 100565, 98684 Ilmenau, Germany, Tel. +49 3677/ 69 3409, Fax. +49 3677/ 69 3355, e-mail: vadim.lebedev@tu-ilmenau.de

Contents

1. LONG-TERM GOALS	2
2. OBJECTIVES	2
3. APPROACH	2
4. WORK COMPLETED.....	3
4.1. AlGaIn/GaN HEMT-based polar liquid sensors for water based nano- and pico-liter droplets	3
4.1.1. Sensor and Application System	3
4.1.2. Liquid Handling and surface modification	4
4.1.3. Sensors, Frames/Peripherals and Electronics	6
4.2. Pt/GaN hydrogen sensors on sapphire.	7
4.3. AlGaIn solar-blind UV photosensors on Si and sapphire substrates: defect related properties...	10
5. PERSONNEL EXCHANGES AND TRAVEL	13
6. RESULTS	13
7. IMPACT/APPLICATIONS	14
8. TRANSITIONS	14
9. RELATED PROJECTS	14
10. RECENT AND RELATED PUBLICATIONS	14

1. LONG-TERM GOALS

Development of novel group III-nitride sensors based on pyroelectric AlGaIn/AlGaIn and AlGaIn/GaN hetero- and nanostructures, including unpassivated HEMT structures for the detection of UV-light, chemical aggressive ions, toxic gases and polar liquids.

2. OBJECTIVES

The potential of pyroelectric AlGaIn/GaN sensors is based on the complex response of polarization induced 2DEGs to variations in the electrostatic boundary conditions of the free surface caused by adsorbed ions, polar liquids and toxic gases. In particular, unpassivated AlGaIn/GaN HEMT structures are used for various kinds of sensors operating in harsh environments such as (1) detectors of the water content in hydraulic oil of actuators, (2) detectors of unwanted emission components from the internal combustion engines (CO , CO_2 , C_xH_y , NO_x) and personal air quality sensors (CO , CO_2), (3) detectors of hydrogen and hydrocarbon species in atmosphere. Catalytic Pd- and Pt-GaN Schottky diodes are employed as hydrogen sensors in clinical, technological, and environmental applications. Solar-blind AlGaIn based UV-photosensors are developed for applications such as flame and heat sensors, ultraviolet calibration devices, plasma diagnostics, engine monitoring, and secure satellite communications. The range of applications also includes the measurement of biologically hazardous UV radiation.

3. APPROACH

The AlGaIn/GaN and GaN sensor heterostructures have been grown on sapphire and pseudo-substrate templates (SiC/Si , AlN/Si , AlN/SiC/Si) epitaxially at the Center for Micro- and Nanotechnologies located at the Technical University Ilmenau and Cornell University (**Prof. L. F. Eastman**). Electron microscopy (TEM and HRTEM) have been applied to the structures at Friedrich-Schiller-University Jena to observe the individual crystal defects and to get quantitative information about strain fields and composition of the epilayers. Analytic studies such as in situ cathodoluminescence (CL), spectral ellipsometry and electron diffraction, Hall-measurements, X-ray

diffraction, Auger electron spectrometry, X-ray photoelectron diffraction (XPS), scanning tunneling microscopy (STM), atomic force microscopy (AFM) have been performed at the TU-Ilmenau to characterize individual AlGa_N and Ga_N layers as well as the completed sensor heterostructures. Testing and optimization methods (sensitivity, dynamic range and noise measurement) of the AlGa_N/Ga_N and Ga_N sensor structures grown on SiC, AlN/Si and SiC/Si composite substrates are under development in a close collaboration between Cornell University and TU Ilmenau. This project is highly collaborative, involving different research groups at TU-Ilmenau, University of Jena (**Dr. U. Kaiser**), Cornell University (**Prof. L. F. Eastman**), IL Metronic GmbH (**Dr. H. Hansch, Dr. W. J. Hummel**), and General Electrics (**V. Tilak and D.W. Merfeld**).

4. WORK COMPLETED

4.1. AlGa_N/Ga_N HEMT-based polar liquid sensors for water based nano- and pico-liter droplets

4.1.1. Sensor and Application System

Miniaturization of analytical and technical devices for biotechnological, medical and chemical applications shows high potential for accelerating the discovery of new biological relevant substances and drugs. Especially nanotechnological approaches promise a new quality with respect to time, sensitivity, and specificity in the field of biology driven sensor technology. New sensor concepts on the nanoscale demand for new system integrative concepts including the manipulation of pico- and nanofluid volumes on chemical or structural modified surfaces and defining suitable interfaces to the macroworld.

A new laboratory build at the Technical University Ilmenau (TUI) with special developed measuring stations (some examples are shown in Fig.1) allow to test several integrative experimental set-ups, which contain new sensors based on AlGa_N/Ga_N heterostructure semiconductor systems, pico- and nanofluidic dispensers based on piezo actuators, the micro periphery and the electronics for measuring biochemical assay systems (in vivo and in vitro). Iterative adaptations of e.g. surface and sensor modifications are performed to find the suitable design for testing the biological systems.

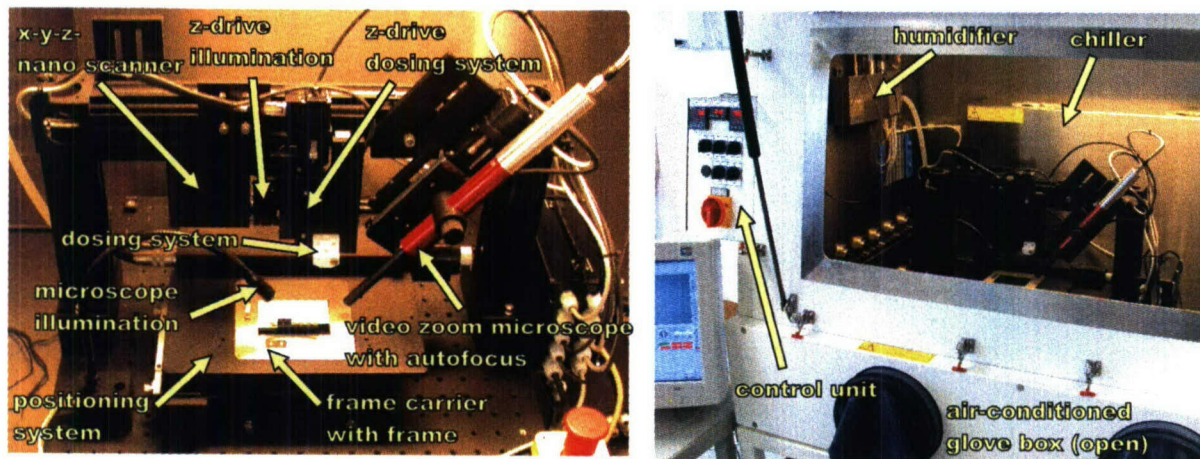


Fig 1: Experimental set-up (left hand side) for dosing and analysis of picoliter droplets including dosing system, positioning system and frame with up to 7 different AlGa_N/Ga_N sensors. Atmospheric chamber (right hand side) with controlled environment by adjusting parameters like relative humidity (1...95%), pressure (± 10 mbar), and temperature (0...60°C).

4.1.2. Liquid Handling and surface modification

The modification and functionalization of GaN and AlGaIn surfaces is an important part of the development of a sensor system analyzing very small volumes of water based liquids in the range of 1 nl down to 50 pl. These small droplets can contain ions, rare substances, expensive pharmaceuticals, and organic substances like viruses. The fluidic system will enable a fast and cheap screening of these substances by electrical and optical measurements. Active liquid handling is realised by using actuators to accelerate or to displace liquids. Different pipetting tools in the range of 50 picoliter with a frequency of 3 kHz up to 10 nanoliters with a frequency of 100 Hz have been developed to place small droplets on the active area of the AlGaIn/GaN sensors (see Fig.2). The silicon dosing systems are piezo driven with a bimorph construction or, alternatively, a piezo stack construction.

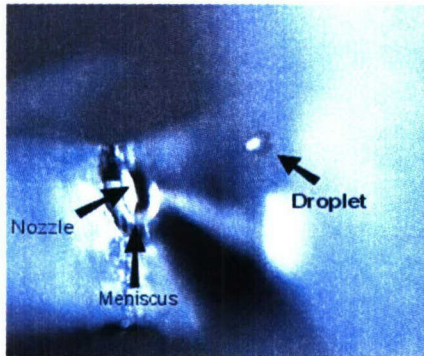


Fig.2: A water based nanodroplet ejected from silicon based dispensing head.

In the second period of the project beside a dosing system a sensor array for analyzing the droplet volume and important physical properties of polar liquids like water was developed. Group III nitrides are the ideal material system to realize the sensor structure. Because of the piezo- and pyroelectric properties AlGaIn/GaN heterostructures can confine a polarization induced two dimensional electron gas (2DEG) close to the interface without the need of a modulation doped barrier. The carrier concentration and electron mobility within the 2DEG can be very high and build up an electrically conductive channel with low sheet resistance. Because of charge neutrality the carrier concentration of the 2DEG is sensitive to any change of net surface charge. As a consequence the source drain current of an AlGaIn/GaN based HEMT structure varies corresponding to a manipulation of surface charge or work function, e.g. caused by polar liquids. The scheme of a sensor is shown in Fig.3. The water droplet will be positioned on the active area and has to spread over the whole sensitive area to achieve a significant drop in source drain current. Therefore a hydrophilic active area and a hydrophobic surrounding are necessary. In addition the dynamic range increases by the proposed manipulation of surface wetting because the 2DEG underneath the whole active area is depleted by small volumes of liquid.

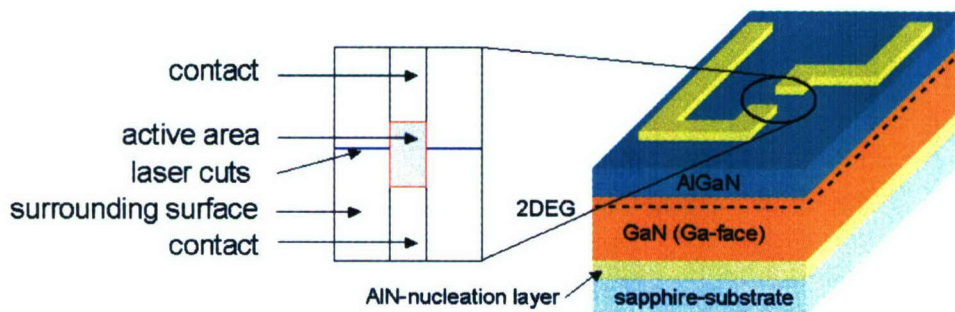


Fig.3: Scheme of a fluidic sensor with enlarged active area and its surrounding.

The third positive effect is the self positioning of droplets over the active area in case of an insufficient droplet positioning. Dry thermal and wet thermal oxidation processes were performed to get a hydrophilic active area. To achieve a hydrophobic surrounding different materials were deposited on top of the sensors and characterized by the methods mentioned above. The dry thermal oxidation was performed by rapid thermal processing (RTP) at about 750°C for 3 minutes under oxygen atmosphere. In all cases the oxidation leads to a better wetting behaviour of the GaN and AlGaN surface. The contact angle of deionized water on GaN decreases from almost 90° to 3° because of a thin oxide layer on top of the sample as revealed by Auger electron spectroscopy (AES). But the wetting behaviour of the oxidized GaN surfaces is not stable in time and as a consequence the contact angle almost increases to the initial value within a few hours. Probably oxygen containing adsorbates, e.g. water, are responsible for this behaviour. Oxidized AlGaN surfaces show a more stable wetting behaviour (Fig.4). The contact angle increases within the first 48 hours, but then keeps stable at 42°. For the wet thermal oxidation a new setup was realized consisting of a quartz tube, a furnace, and a bubbler. Experiments by wet oxidation of GaN samples revealed a similar characteristic like for dry oxidation. The wetting behaviour was drastically improved but degraded with time. SiN_x, oxidized aluminium, and fluorine carbon compounds (FC) were deposited on the sensor to realize a hydrophobic active area, but only fluorine-carbon (FC) compounds had hydrophobic properties as it is shown in Fig.5. FC layers were deposited by reactive ion etching (RIE) or by inductively coupled plasma (ICP) processes.



Fig.4: Water droplet on hydrophilic oxidized AlGaN surface

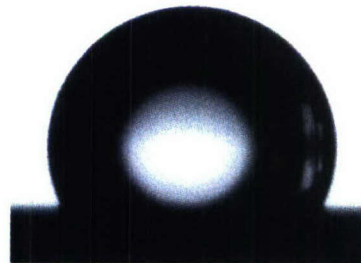


Fig.5: Water droplet on ICP Fluorine-Carbon layer.

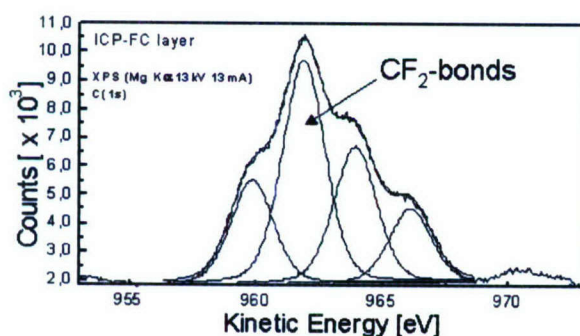


Fig.6: XPS measurement for an ICP-FC layer.

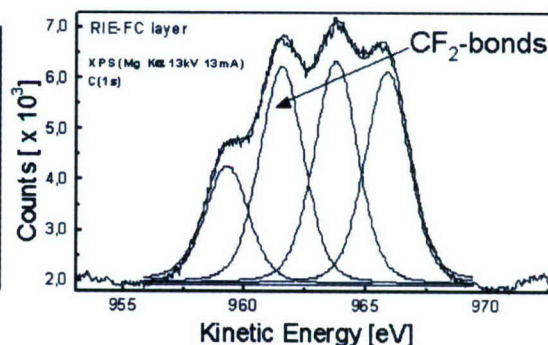


Fig.7: XPS measurement for a RIE-FC layer.

The FC layers had different wetting properties in dependence of processing because of different chemical composition. The ICP layers had a higher content of CF₂-bonds (Figs.6 and 7). These bonds are responsible for the hydrophobic behaviour as it is known from PTFE (Teflon®) which consists of

CF₂-bonds. FC layers also showed an instable wetting behaviour, but after 6 hours the contact angle remained stable.

The next step was the electrical characterization of the thin FC layers. After deposition on an insulating substrate (sapphire) gold contacts were evaporated on the FC layer. The specific resistance and conductivity were calculated by taking into account the film thickness and contact geometry. The specific resistance of the FC layers is in the range of 1.6×10^9 to 8×10^{10} Ohm*cm (Tab.1) and is two orders of magnitude higher than that of deionized water. So a current path through this layers is avoided. The last step was to check whether it was possible to create a window for the active area in the FC layers and to passivate the contacts by FC layers. The critical dimension is about 5 μ m. It was successfully realized by a lift-off process. Dry thermal oxidation of AlGaN surfaces leads to an improved and stable wetting behaviour of the active area. Fluorine-carbon layers are used to successfully realize a hydrophobic surrounding. Further work will show the influence of surface modification on the electrical characteristic of the sensor and will lead to a better understanding of the oxidation process.

Tab. 1: Electrical properties of the hydrophobic ICP fluorine-carbon-compound layer.

	RIE FC-layer	ICP FC- layer	DI-water
Resistivity [Ohm*cm]	8×10^{10}	1.6×10^9	2×10^7
Conductivity [S/cm]	1.2×10^{-11}	6.2×10^{-10}	5×10^{-8}

4.1.3. Sensors, Frames/Peripherals and Electronics

AlGaN/GaN-heterostructure semiconductor devices were produced by plasma induced molecular beam epitaxy (PIMBE). Metallisation of source- and drain contacts was realized. First sensors arrays were constructed. The important electronic parameters e.g. the transport parameters of the Al_xGa_{1-x}N-layers could be simulated and identified by the bound/interface charge model and the two dimensional electron gas (2DEG) mobility model serving as tools for developing optimal sensor geometries. Based on the functional requirements for the sensors two different designs and materials of the frames for the integration of up to seven different sensors into a sensor array have been developed. The frame made of silicon is bonded onto a borosilicate base plate structured by micro sand blasting. Each sensor will be fixed by spring clamping allowing easy replacement of the sensors. The silicon is constructed by anisotropic etching. A titan gold layer enables bond and soldering processes. The frame made of LTCC (low temperature cofired ceramics) has been constructed for fluid application with pH values > 7. It consists of 5 layers, which have been constructed by UV Laser radiation in the green state before sintering. The lamination and sintering process was optimized with respect to crack initiation and forming, which results in suitable frame configurations for the sensors (Fig. 8b).

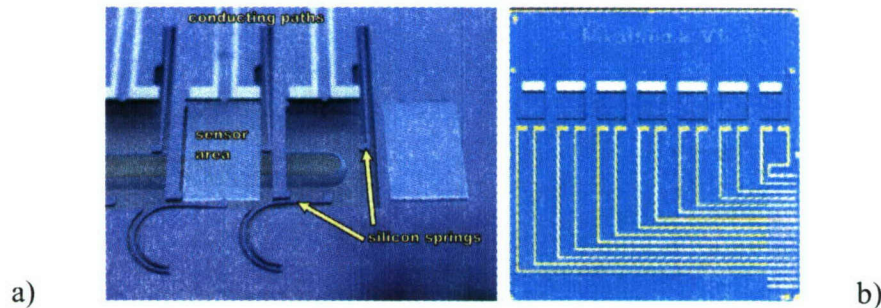


Fig.8: (a) Silicon frame with the spring structure (b) frame made of LTCC.

By integration of an electronic read out system (Agilent) consisting of a parameter analyzer with a high power source monitor unit (SMU), two mid power SMUs and a 10x12 matrix switch, first measurements with the sensors have been performed (Fig. 9, 10). The size of a water droplet is determined by the change of the source drain current with the time during evaporation of the droplet.

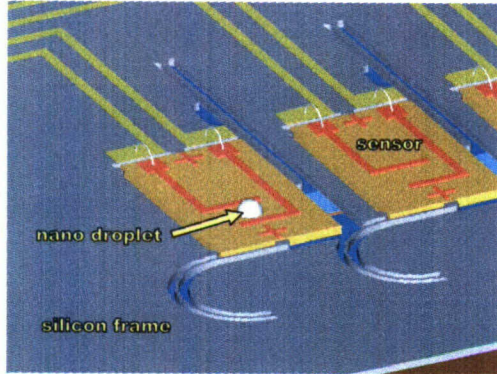


Fig.9: AlGaIn/GaN sensor with nano droplet on top embedded into the Si frame including contacts.

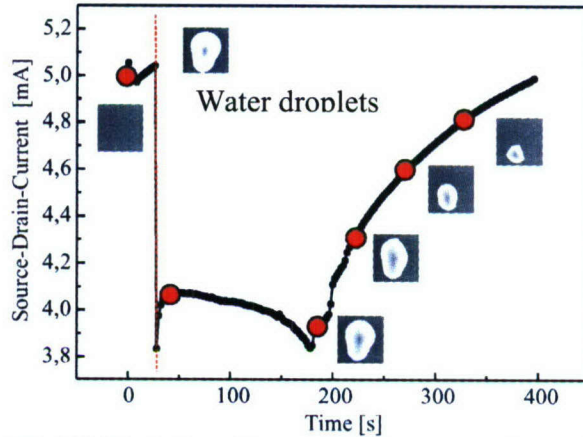


Fig.10: Variation of source drain current due to the positioning and evaporation of a water droplet on top of the active sensor area.

First experiments according to the influence of AlGaIn surfaces to biological materials have been performed. The biocompatibility of the semiconductor heterostructure is analyzed by cell adherence. Cell growth on this material is examined and shows – as a first result – no strong interference. Further research will be focused on the optimization of the sensors and the experimental set- up with respect to the biological material.

4.2. Pt/GaN hydrogen sensors on sapphire.

The use of hydrogen gas has gained a considerable attention in industrial fabrication processes, medical installations, laboratories and fuelled motor vehicles. For safety reasons the monitoring of hydrogen molecules has become an important issue. One up to date technical solution to realize sensitive sensors for hydrogen and hydrocarbon gases in air is the combination of catalytic metals (Pd or Pt) with wide band gap semiconductors like GaN. At the Pt surface molecular hydrogen is dissociated into atomic hydrogen atoms which are able to diffuse very fast towards the Pt/GaN interface. Hydrogen accumulation at the interface changes the work function of the metal gate and therefore the barrier height of the Schottky contact which can be proven by measuring I-V curves.

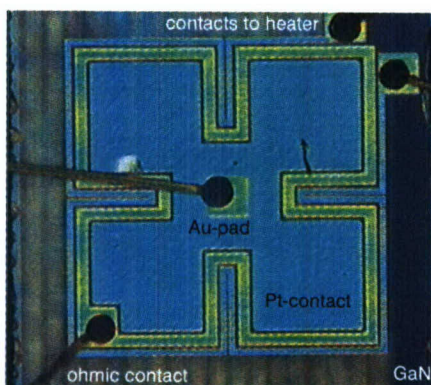


Fig.11: Top-view micrograph of the Pt/GaN Schottky Diode processed by General Electric. The active area of the device is about 1 mm².

The sensors were prepared on GaN layers grown by metal organic chemical vapor deposition (MOCVD) on sapphire substrates. The thickness of the epitaxial GaN layer was about 3 μm , the n-type doping concentration around $\sim 1 \cdot 10^{17} \text{ cm}^{-3}$. The thickness of the Pt-Schottky contact was varied between 8 and 40 nm and the size of the active sensor area between 0.25 and 1 mm^2 (Fig.11). The sensor structure was placed into a TO transistor package with an integrated heater. The sensitivity, response and recovery times have been measured for the different designs of Pt/GaN sensors as follows. I-V curves were recorded in dependence on the operating temperature in synthetic air as well as in synthetic air containing 1 vol% hydrogen gas. As shown in (Fig.12) exposure of Pt/GaN Schottky diodes to H_2 causes an increase of both the forward and reverse current which can be attributed to a decrease in the Schottky barrier height. In a constant current operation mode this reduction of the Schottky barrier height results in a shift to lower bias voltages, which constitutes the sensor signal.

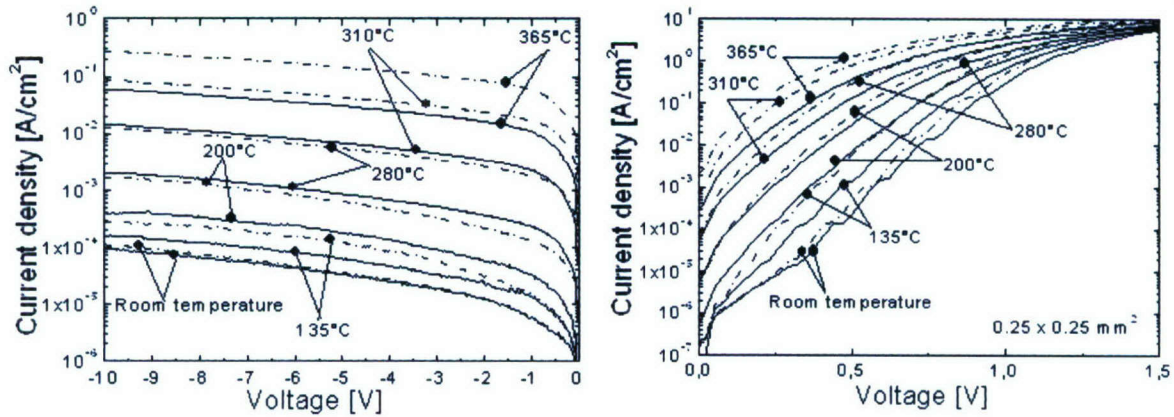


Fig.12: I-V curves of the Pt/GaN Schottky diodes operated at different temperatures and in synthetic air (solid lines) or in synthetic air with 1 vol% hydrogen gas (dashed curves, ($d_{\text{Pt}} = 24 \text{ nm}$)).

The sensitivity to H_2 was investigated in dependence on the active area, Pt thickness and the operating temperature. The change in the voltage of the diode at a fixed current was monitored as the diode was exposed to 1% H_2 in synthetic air and for comparison to dry synthetic air in order to determine the voltage difference as a measure for the sensitivity towards hydrogen gas.

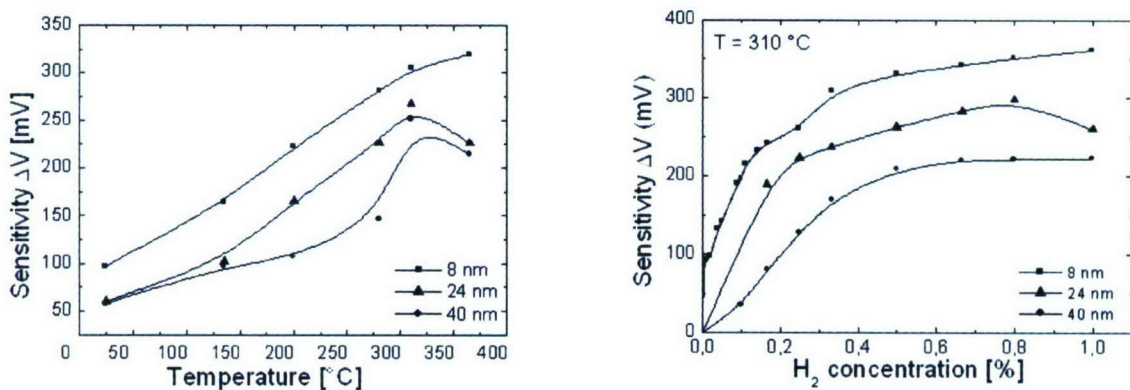


Fig.13: Sensitivity of the Pt/GaN Schottky diodes in constant current density mode ($J = 3.2 \text{ A/cm}^2$) for different thickness a) at different operation temperatures. b) for different concentrations of hydrogen gas. ($A_{\text{Pt}} = 250 \times 250 \mu\text{m}^2$). The sensitivity of the detector is given by $\Delta V = V_{\text{air}} - V_{\text{hydrogen}}$.

The significant increase of sensitivity by increasing the temperature of operation to $\sim 365^\circ\text{C}$ and by decreasing the Pt thickness down to 80 \AA has been observed (Fig.13). An expected voltage drop after the sensor is exposed to hydrogen has been measured due to the reduction in Schottky barrier height. We have also found that the sensitivity increases non linear with an increasing concentration of H_2 in air starting from 0.1 vol% to 1 vol% for all Pt contact thickness.

The micro-structure of Pt contacts was studied by means of electron microscopy (in terms of grain boundary density and average grain size). As expected, the higher sensitivity films have also a higher grain boundary density proving that hydrogen molecules dissociate on the Pt surface and diffuse along

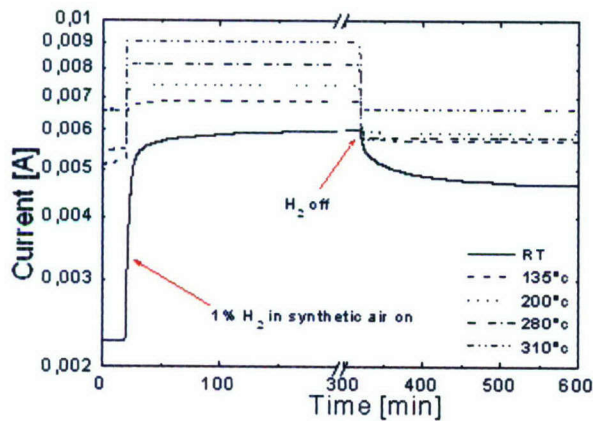


Fig.14: Transient behaviour of electrical response of a sensor with an active area of $0.5 \times 0.5 \text{ mm}^2$ exposed to 1 vol% H_2 in synthetic air at different temperatures, $d_{\text{Pt}} = 24 \text{ nm}$.

the grain boundaries reaching the Pt/GaN interface. A transient behaviour of electrical response of $0.5 \times 0.5 \text{ mm}^2$ sensors operated in constant voltage mode ($U = 1 \text{ V}$) and exposed to a 1 vol% H_2 in synthetic air pulse is observed at different temperatures (Fig. 14).

The response (diffusion) times at room temperature were more than 1 hour and the recovery times were also very long, typically several hours. The long recovery time of Pt/GaN Schottky contacts after exposure to H_2 at room temperature indicates a strong trapping of hydrogen atoms at electronically active adsorption sites. We observed a significant decrease of response and recovery time by decreasing the Pt thickness down to 8 nm and by increasing the operation temperature to 365°C (Fig.14).

Conclusions:

- (1) The sensitivity to hydrogen gas was observed down to room temperature. An effective sensor operation at room temperature is possible.
- (2) The sensitivity significantly improves with increasing operation temperatures. An excellent stability of the catalytic layer and the interface up to 400°C was proven.
- (3) For thinner catalytic contact layers (down to 8 nm) the sensitivity is increased. A significant decrease in response and recovery time (up to several seconds) by the decreasing the Pt thickness and by increasing the operation temperature to $\sim 365^\circ\text{C}$ has been realized.

4.3. AlGaN solar-blind UV photosensors on Si and sapphire substrates: defect related properties.

The unique intrinsic properties and remarkable progress in the epitaxial growth of high-quality III-nitrides films have given rise to successful commercialization of group III nitride based optoelectronic devices. A large variation in the band gap energies and the ability to form heterojunctions have made $\text{Al}_x\text{Ga}_{1-x}\text{N}$ alloys the most adequate and flexible solution for UV light detection.

AlGaN-based solar blind UV-detectors with integrated filter having high responsivities in a narrow range of photon energies were grown by MBE on sapphire and SiC(111)/Si(111) epitaxial templates. This detector structure has been designed for the UV monitoring of biologically active species in the drink-water purification process (see also 12th month progress report for detectors grown on sapphire).

Despite of the rapid development in the growth techniques, the major problem of AlGaN layers is the presence of defects in large quantities, which are generated during the heteroepitaxy and post-epitaxial treatment. The detailed knowledge of the defect structure is highly desirable for improvements of AlGaN based devices. In this work, a combination of room temperature *in-situ* cathodoluminescence (CL), photocurrent spectroscopy (SPC) and spectral ellipsometry (SE) have been applied to study defect-related absorption and emission in AlGaN-based photodetectors designed for a high responsivity in a narrow spectral range (240-300 nm, $\lambda_{\text{peak}} = 280$ nm). Nominally undoped epitaxial $\text{Al}_x\text{Ga}_{1-x}\text{N}$ heterostructures were grown on *c*- Al_2O_3 substrates by molecular beam epitaxy. Firstly, an $\text{Al}_{0.67}\text{Ga}_{0.33}\text{N}$ optical filter layer ($E_g \sim 4.8$ eV, $d \sim 0.2$ μm) has been grown on sapphire coated with an AlN nucleation layer ($d \sim 40$ nm). This layer is absorbing photons with energies above 4.8 eV and acts as a high photon energy filter. An AlN epilayer ($d \sim 100$ nm) was grown as an insulating barrier ($E_g = 6.2$ eV) on top. Finally, a 0.3 μm thick $\text{Al}_{0.48}\text{Ga}_{0.52}\text{N}$ capping layer ($E_g \sim 4.4$ eV) has been grown acting as UV photoconductor collecting photons with energies in the range of 4.4 to 4.8 eV.

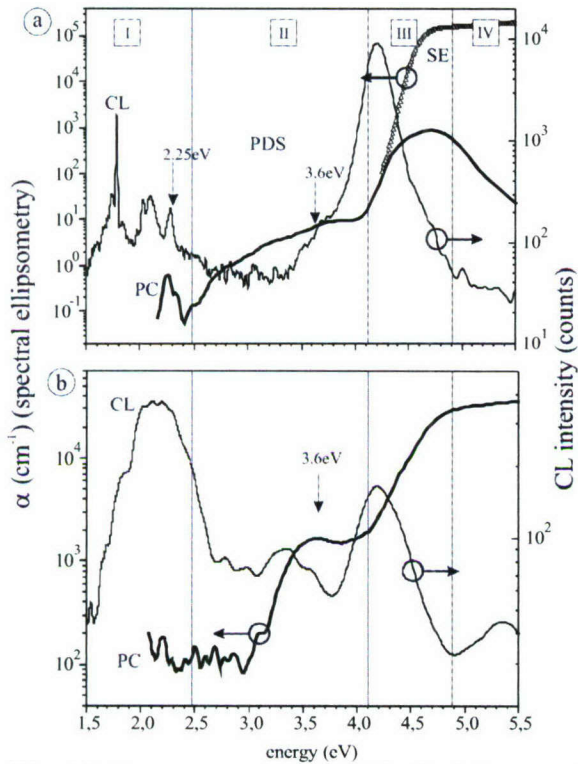


Fig. 15: Room temperature SPC (thick line) and *in-situ* CL spectra of (a) the detector structure grown on sapphire, and (b) the detector layer grown on Si(111). The curve marked by open triangles represent the absorption coefficient α given by spectral ellipsometry.

200 to 400 μm have been used for electronic measurement. In Fig.15(a,b) the CL, SPC and SE curves measured on UV-detectors are presented. Despite of the UV/visible contrast of more than four orders of magnitude, the obvious responsivity has been observed in the SPC spectra well below the band gap (< 4 eV). The low-energy SPC absorption is dominant by a broad photoionization shoulder with an

UV-detectors based on Si(111) substrates have been deposited at similar growth conditions and consisted of the buffer and detector layers without the integrated filter. Surface related silicon has been detected by AES, while the residual Si doping was measured in the bulk by SIMS. The detector devices were processed by a conventional photolithography. Samples with Ti/Al (20/80 nm) finger contacts with a contact spacing ranging from

onset of ~ 2.5 eV usually attributed to the transitions from various deep defect states to the levels above the mobility edge of the conduction band (Fig.15a, zone II) as well as a resonant SPC peak at ~ 2.25 eV (Fig.15a, zone I). The latter peak correlates well with the CL peak at the same energy position. It is usually associated with transitions from a shallow donor (SD) to a very deep acceptor (DA). Due to its resonance nature, the SPC peak centred at 2.25 eV cannot be attributed to the direct photoionization. It contributes to the SPC by means of the internal optical excitation between a mid-gap state and a localized SD state with $E_A \sim kT$ at 300 K followed by the thermal ionisation. An acceptor character at least of some of the very deep levels (V_{Ga} , carbon) has been predicted. Because the acceptor levels in n -type nitrides have been never experimentally observed, we can relate this resonance peak to DA transitions with $E_A^e \sim 2.2$ eV. The effective value of the activation energy for the shallow level is $E_A = 86 \pm 5$ meV. Dominant donors in intentionally undoped III-nitrides are Si and O. Oxygen is a dominant impurity in the undoped $Al_xGa_{1-x}N$ epilayers. Theoretical calculations predict that oxygen can occupy a substitutional nitrogen site O_N forming a localized shallow donor state ($E_A \sim 14$ meV for $x \sim 0.4$). In the $AlGaN/AlN/Si$ heterostructures, unintentional silicon doping is of great importance due to the strong silicon out-diffusion and channelling via the grain boundaries between AlN domains. Si also creates a SD level corresponding to the Si localized state with a DX-center behaviour with $E_A \sim 30$ meV for $x \sim 0.5$. Taking into account the spreading of the localized states due to the potential fluctuations and alloy effects, we conclude that both states (O_N and Si^{DX}) can contribute to the resonance SPC peaks at 300 K.

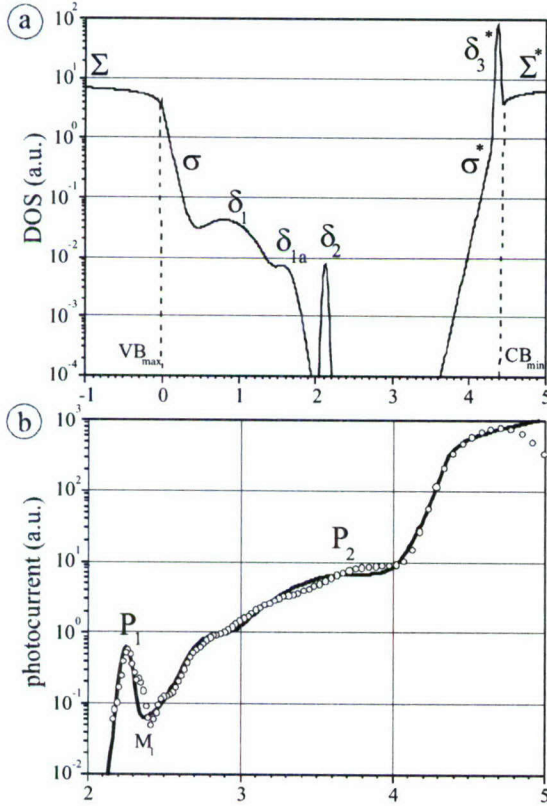


Fig.16: (a) Proposed non-equilibrium DOS model for $AlGaN$. Empty states are indicated by (*). (b) SPC absorption fit for the layer grown on sapphire, (open circles: SPC experiment, solid line: simulation).

A broad SPC shoulder with an onset of ~ 2.5 eV (Fig.15a, zone II) can be described as a photoionization process from the impurity related deep levels either onto SD level or into the CB. Due to the large activation energies and residual n -type conductivity of the epilayers, it can be attributed to the wide DA band. SPC spectra of high quality samples

grown on sapphire do not show any remarkable features in this spectral region (Fig.15a) except an unpronounced shoulder with an onset of ~ 3.5 eV. On the other hand, SPC and CL spectra measured on the $AlGaN/AlN/Si$ structures reveal that the second resonance peak centred at the same position (~ 3.6 eV) dominates the subband absorption and emission (Fig.15b). The resonance nature of the absorption peak is also obvious, similar to the absorption peak at 2.25 eV assuming the existence of at least two localized states: already mentioned SD (Si^{DX} or O_N) and DA with a hole activation energy of ~ 0.8 eV. It was also predicted that carbon incorporated substitutional on the nitrogen site gives rise to an acceptor in GaN and AlN . In the latter case, C_N becomes a deep acceptor introducing the localized energy level at ~ 0.9 eV above the valence band. These predictions are in a good agreement with our spectral and AES observations allowing to consider C_N related states participating in the absorption

shoulder (onset of $\sim 3.5\text{eV}$, Fig.15a, zone II). The AlGa_{0.33}N sub-band absorption and emission are extremely difficult for interpretation due to the large number of the bands involved in the SPC and CL transitions. However, at least a qualitative density of states (DOS) model can be derived from our SPC measurements based on the positions of the resonance features observed (see Fig. 16). The simulation shows very good fit to the experimental data.

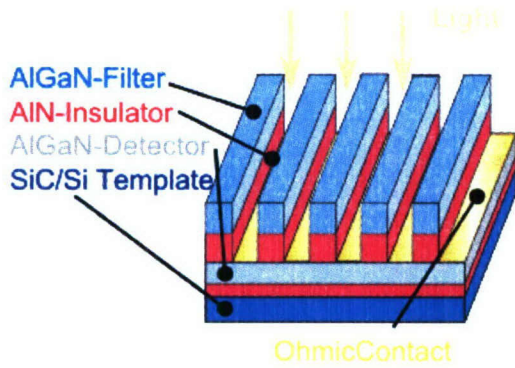


Fig. 17. Schematic representation of the AlGa_{0.33}N based UV-detector structure with integrated filter on Si/SiC template.

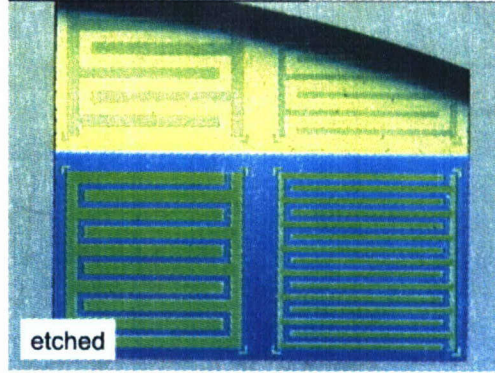


Fig. 18. Top-view of the processed AlGa_{0.33}N UV-detector.

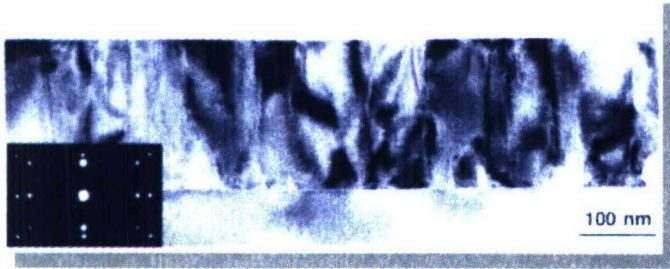


Fig. 19. Bright-field TEM micrograph of 2H-AlN(0001)/SiC(111)/Si(111) structure used as a template for UV detector growth.

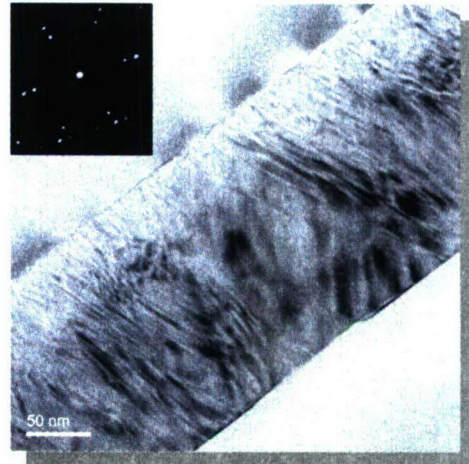


Fig. 20. Bright-field TEM micrograph of cubic 3C-AlN(111)/SiC(111)/Si(111) epitaxial template.

Summary: The AlGa_{0.33}N based UV-detectors with integrated filter have been grown on sapphire and Si/SiC templates. For the latter detectors (Fig. 17, 19, 20), the UV/visible contrast of more than three orders of magnitude has been observed. For the dry etching of the AlGa_{0.33}N structures, a modified ECR-plasma etching system has been used equipped with dual gas-inlet-system for working gases (Ar, O₂) and C₂H₄ and H₂ mixture. The iso- and anisotropical etch process has been developed for AlGa_{0.33}N and GaN structures (Fig. 18).

The achieved parameters of the device:

- Spectral response: $\lambda = 240 - 300 \text{ nm}$,
- UV/visible contrast $> 10^3$,
- Integrated Al_{0.67}Ga_{0.33}N filter for $\lambda < 240 \text{ nm}$,

- Background doping (n-type) $< 1 \cdot 10^{17} \text{ cm}^{-3}$
- Lifetime $> 1000 \text{ h}$
- Reliable linearity behavior up to 40 V

5. PERSONNEL EXCHANGES AND TRAVEL

Tab.2. Summary of personnel exchanges and travel conducted under this NICOP (month 12 to 18 of the project).

NAME	HOME INSTITUTION	INSTITUTION / LOCATION VISITED	SCIENTIFIC / TECHNICAL PURPOSE OF VISIT	DATES (MM/DD/YY)
Vadim Lebedev	TU-Ilmenau	Montpellier, France	Inter. Conference	06/2004, 5 days
Volker Cimalla	TU-Ilmenau	Gabelbach, Germany	Workshop Biotechnology and Microreaction Techniques	01/2004 3 days
Gabriel Kittler	TU-Ilmenau	Gabelbach, Germany	Workshop Biotechnology and Microreaction Techniques	01/2004 3 days
Thomas Stauden	TU-Ilmenau (Staff)	Infineon AG, Munich, Germany	Transport of equipment for NICOP project	12/2003 2 days

Other travel / exchange assisted by ONR program: no

6. RESULTS

1. Pyroelectric 2DEG $\text{Al}_x\text{Ga}_{1-x}\text{N}/\text{GaN}$ ($x = 22, 33 \%$, $\mu \sim 1400 \text{ cm}^2\text{V}^{-1}\text{sec}^{-1}$, $N_{2\text{DEG}} \sim 1.5 \times 10^{13} \text{ cm}^{-2}$) sensor structures have been fabricated at TU-Ilmenau using the hydrophobic fluorine-carbon-compound cap layer. The structures with $500 \times 500 \mu\text{m}^2$ active area have demonstrated good electrical characteristics, large dynamic range ($\sim 1.2 \text{ mA}$) and good sensitivity to polar liquid micro-droplets (water, acetate).
2. A sensor array was realized combining up to seven independent and different sensors inside a Si- or LTCC-frame for analysis of water based nano- and picoliter droplets. This sensor array is already combined with a positioning and dosing system for high throughput screening of organic materials carried by droplets.
3. A new series of the Pt/GaN hydrogen sensors have demonstrated an excellent sensitivity to hydrogen at 350°C ($\Delta V > 180 \text{ mV}$, $\Delta V = V_{\text{air}} - V_{\text{hydrogen}}$) and with a good stability of the catalytic layer and the interface. The sensor with 80 \AA thin catalytic contact layer has demonstrated an acceptable sensitivity already at room temperature. However, a further decrease in response and recovery time (up to several seconds) is required to make the sensors efficient for the practical use.

4. AlGaN-based solar blind UV-detectors with integrated filter having high responsivities in a narrow range of photon energies were grown by PIMBE on **Si(111)** substrates. The performance of the sensors grown on Si is comparable with those grown on sapphire substrates:
 Spectral response: $\lambda = 240 - 300 \text{ nm}$,
 UV/visible contrast $> 10^3$,
 Integrated $\text{Al}_{0.67}\text{Ga}_{0.33}\text{N}$ filter for $\lambda < 240 \text{ nm}$,
 Background doping (n-type) $< 1 \cdot 10^{17} \text{ cm}^{-3}$,
 Lifetime $> 1000 \text{ h}$,
 Reliable linearity behavior up to 40 V.
5. For the dry etching of the AlGaN structures, a modified ECR-plasma etching process has been developed using dual gas-inlet-system for working gases (Ar , O_2) and C_2H_4 and H_2 mixture. The iso- and anisotropical etch process has been developed for AlGaN and GaN structures.

7. IMPACT/APPLICATIONS

1. AlGaN/SiC/Si solar-blind, selective photodetectors with an integrated optical filter have been designed and processed (sensitive in the range $\lambda = 240 - 300 \text{ nm}$). The detector structure is designed for the UV monitoring of biologically active species in the drinking water purification process.
2. The pyroelectric AlGaN/GaN sensor structure with 2DEG has been fabricated using the hydrophobic fluorine-carbon-compound cap layer. The first structures with $500 \times 500 \mu\text{m}^2$ active area have been designed for measurements of the micro-liter polar-molecule liquid droplets.

8. TRANSITIONS

-

9. RELATED PROJECTS

1. “New generation of GaN based sensor arrays for nano- and pico-fluidic systems for fast and reliable biomedical testing”, funded by the European Commission, Call identifier FP6-2002-NMP-1, Proposal No.: STRP 505641-1 GaNano.
2. “Zell- und Biomolekül-Sensoren in Piko- und Nanofluidischen Systemen“, funded by Freistaat Thüringen, Proposal No.: B 678-03001 Picofluidik.

10. RECENT AND RELATED PUBLICATIONS

Epitaxial stabilization of cubic AlN polytype on 3C-SiC/Si(111) templates

Vadim Lebedev, Christian Förster, Ute Kaiser, Volker Cimalla, Jörg Pezoldt, Johannes Biskupek and Oliver Ambacher, submitted to Appl. Phys. Lett. (2004).

Defect related absorption and emission in AlGaN solar-blind UV photodetectors

V. Lebedev, I. Cimalla, V. Cimalla, R. Wagner, U. Kaiser and O. Ambacher, phys. stat. sol. (c), in print (2004).

Gap state absorption in AlGa_N photoconductors and solar-blind photodetectors
V. Lebedev, I. Cimalla, U. Kaiser and O. Ambacher phys. stat. sol. (c) 1-5 (2004).

Investigations of MBE grown InN and the influence of sputtering on the surface composition,
R. Krischok, V. Yanev, O. Balykov, M. Himmerlich, J.A. Schäfer, R. Kosiba, G. Ecke, I. Cimalla, V. Cimalla, O. Ambacher, H. Lu, W.J. Schaff, and L.F. Eastman,
Surface Science (2004) submitted.

Recent advances in GaN HEMT development
F. Schwierz and O. Ambacher
J. Appl. Phys. (2004) submitted.

Study of pinholes and nanotubes in AlInGa_N films by cathodoluminescence and atomic force microscopy,
H. Herrera, A. Cremades, J. Piqueras, M. Stutzmann, O. Ambacher,
J. Appl. Phys. **95** (2004) 5305.

Photoreflectance studies of Al(Ga)- and N-face AlGa_N/Ga_N heterostructures,
C. Buchheim, A.T. Winzer, R. Goldhahn, G. Gobsch, O. Ambacher, A. Link, M. Eickhoff,
M. Stutzmann, Thin Solid Films **450** (2004) 155.

Temperature dependent electric fields in Ga_N Schottky diodes studied by electrophotoreflectance,
R. Shokhovets, D. Fuhrmann, R. Goldhahn, G. Gobsch, O. Ambacher, M. Hermann, M. Eickhoff, Thin
Solid Films **450** (2004) 163.

Sputter depth profiling of InN layers,
R. Kosiba, G. Ecke, V. Cimalla, L. Spieß, and O. Ambacher
Nuclear Instruments and Methods in Physics Research B **215** (2004) 486.

Growth of a-plane InN on r-plane sapphire with a Ga_N buffer by molecular-beam epitaxy,
H. Lu, W. J. Schaff, L. F. Eastman, J. Wu, W. Walukiewicz, V. Cimalla, and O. Ambacher,
Appl. Phys. Lett. **83** (2003) 1136.

Photoreflectance studies of N- and Ga-face AlGa_N/Ga_N heterostructures confining a polarisation induced 2DEG
A.T. Winzer, R. Goldhahn, C. Buchheim, O. Ambacher, A. Link, M. Stutzmann, Y. Smorchkova, U.K. Mishra, and J.S. Speck, phys. stat. sol. (b) **240** (2003) 380.

Electronics and Sensors Based on Pyroelectric AlGa_N/Ga_N Heterostructures,
Part A: Polarization and Pyroelectronics,
O. Ambacher, M. Eickhoff, A. Link, M. Hermann, M. Stutzmann, F. Bernardini, V. Fiorentini, Y. Smorchkova, J. Speck, U. Mishra, W. Scharff, V. Tilak, and L. F. Eastman,
phys. stat. sol. (c) **0** (2003) 1878.

PART B: Sensor Applications,

M. Eickhoff, J. Schalwig, O. Weidmann, L. Görgens, R. Neuberger, M. Hermann, G. Steinhoff, B. Baur, G. Müller, O. Ambacher, and M. Stutzmann, *phys. stat. sol. (c)* **0** (2003) 1908.

Recent Presentations on Conferences and Workshops

1. G. Kittler, V. Cimalla, V. Lebedev, M. Fischer, S. Krischok, V. Yanev, J. A. Schaefer and O. Ambacher, "Modification of GaN and AlGa_N Surfaces for Nano- and Picofluidic Sensors", EMRS-2004 (2004).
2. O. Ambacher, "Electronic Transport Properties of Polarization Induced 2DEGs", ONR-Workshop, Monterey, CA, August 5-8, 2004.
3. V. Lebedev, I. Cimalla and O. Ambacher, "Studies on sub-band gap absorption in AlGa_N photoconductors and solar-blind photodetectors", E-MRS-2003 Spring Meeting (2003).
4. I. Cimalla, V. Lebedev, V. Cimalla, and O. Ambacher, "Investigation of the absorption behaviour of thin layers of group III nitrides by Photothermal Deflection Spectroscopy and Constant Photocurrent Measurement ", DPG Frühjahrstagung, Dresden, Germany (2003) HL.

17th of August 2004, at TU-Ilmenau.

REPORT DOCUMENTATION PAGEForm Approved
OMB No. 0704-0188

Public reporting burden for this collection of information is estimated to average 1 hour per response, including the time for reviewing instructions, searching data sources, gathering and maintaining the data needed, and completing and reviewing the collection of information. Send comments regarding this burden estimate or any other aspect of this collection of information, including suggestions for reducing this burden to Washington Headquarters Service, Directorate for Information Operations and Reports, 1215 Jefferson Davis Highway, Suite 1204, Arlington, VA 22202-4302, and to the Office of Management and Budget, Paperwork Reduction Project (0704-0188) Washington, DC 20503.

PLEASE DO NOT RETURN YOUR FORM TO THE ABOVE ADDRESS.

1. REPORT DATE (DD-MM-YYYY) 17.08.2004		2. REPORT DATE 18th mon. progress report		3. DATES COVERED (From - To) 01.01.2004-31.07.2004	
4. TITLE AND SUBTITLE Pyroelectric AlGaIn/GaN HEMTs for ion-, gas- and polar-liquid sensors				5a. CONTRACT NUMBER -	
				5b. GRANT NUMBER N00014-03-1-0301	
6. AUTHOR(S) AMBACHER, Oliver, Prof. Pl. LEBEDEV, Vadim, Dr.				5c. PROGRAM ELEMENT NUMBER -	
				5d. PROJECT NUMBER 03PRO5145-00	
7. PERFORMING ORGANIZATION NAME(S) AND ADDRESS(ES) Technical University Ilmenau, Center for Micro- and Nanotechnologies, PO 100565, 98684 Ilmenau, Germany, e-mail: oliver.ambacher@tu-ilmenau.de				5e. TASK NUMBER -	
				5f. WORK UNIT NUMBER -	
9. SPONSORING/MONITORING AGENCY NAME(S) AND ADDRESS(ES) OFFICE OF NAVAL RESEARCH BALLSTON CENTRE TOWER ONE, 800 NORTH QUINCY STREET, ARLINGTON VA 22217-5660				8. PERFORMING ORGANIZATION REPORT NUMBER NICOP-2-2003-APR	
				10. SPONSOR/MONITOR'S ACRONYM(S) ONR	
12. DISTRIBUTION AVAILABILITY STATEMENT no agency-mandated availability statements				11. SPONSORING/MONITORING AGENCY REPORT NUMBER -	
13. SUPPLEMENTARY NOTES no					
14. ABSTRACT The 18th month progress report includes the results on processing and investigations of (1) pyroelectric HEMT based sensors for polar-liquid molecules detection; (2) Pt GaN Schottky diode hydrogen sensors; (3) AlGaIn/Si-based solar-blind UV photosensors. Summary of the results: (1) the AlGaIn/GaN HEMT sensors have been processed and tested with water and acetate pica-droplets. (2) Pt/GaN catalytic hydrogen sensors were processed and tested to operate at 350°C and RT. (3) high-performance AlGaIn solar-blind UV photosensors with a spectral response of 240 - 300 nm and UV/visible contrast > 10e3 have been grown on Si substrates.					
15. SUBJECT TERMS HEMT, SENSOR, III-NITRIDES, AlGaIn, GaN, UV DETECTOR, SCHOTTKY DIODE					
16. SECURITY CLASSIFICATION OF:			17. LIMITATION OF ABSTRACT	18. NUMBER OF PAGES	19a. NAME OF RESPONSIBLE PERSON
a. REPORT	b. ABSTRACT	c. THIS PAGE			Dr Vadim Lebedev
-	-	-	UU	9	19b. TELEPHONE NUMBER (Include area code) +49 3677 693410

INSTRUCTIONS FOR COMPLETING SF 298

1. REPORT DATE. Full publication date, including day, month, if available. Must cite at least the year and be Year 2000 compliant, e.g., 30-06-1998; xx-08-1998; xx-xx-1998.

2. REPORT TYPE. State the type of report, such as final, technical, interim, memorandum, master's thesis, progress, quarterly, research, special, group study, etc.

3. DATES COVERED. Indicate the time during which the work was performed and the report was written, e.g., Jun 1997 - Jun 1998; 1-10 Jun 1996; May - Nov 1998; Nov 1998.

4. TITLE. Enter title and subtitle with volume number and part number, if applicable. On classified documents, enter the title classification in parentheses.

5a. CONTRACT NUMBER. Enter all contract numbers as they appear in the report, e.g. F33615-86-C-5169.

5b. GRANT NUMBER. Enter all grant numbers as they appear in the report, e.g. 1F665702D1257.

5c. PROGRAM ELEMENT NUMBER. Enter all program element numbers as they appear in the report, e.g. AFOSR-82-1234.

5d. PROJECT NUMBER. Enter all project numbers as they appear in the report, e.g. 1F665702D1257; ILIR.

5e. TASK NUMBER. Enter all task numbers as they appear in the report, e.g. 05; RF0330201; T4112.

5f. WORK UNIT NUMBER. Enter all work unit numbers as they appear in the report, e.g. 001; AFAPL30480105.

6. AUTHOR(S). Enter name(s) of person(s) responsible for writing the report, performing the research, or credited with the content of the report. The form of entry is the last name, first name, middle initial, and additional qualifiers separated by commas, e.g. Smith, Richard, Jr.

7. PERFORMING ORGANIZATION NAME(S) AND ADDRESS(ES). Self-explanatory.

8. PERFORMING ORGANIZATION REPORT NUMBER.

Enter all unique alphanumeric report numbers assigned by the performing organization, e.g. BRL-1234; AFWL-TR-85-4017-Vol-21-PT-2.

9. SPONSORING/MONITORING AGENCY NAME(S)

AND ADDRESS(ES). Enter the name and address of the organization(s) financially responsible for and monitoring the work.

10. SPONSOR/MONITOR'S ACRONYM(S). Enter, if available, e.g. BRL, ARDEC, NADC.

11. SPONSOR/MONITOR'S REPORT NUMBER(S).

Enter report number as assigned by the sponsoring/monitoring agency, if available, e.g. BRL-TR-829; -215.

12. DISTRIBUTION/AVAILABILITY STATEMENT. Use

agency-mandated availability statements to indicate the public availability or distribution limitations of the report. If additional limitations/restrictions or special markings are indicated, follow agency authorization procedures, e.g. RD/FRD, PROPIN, ITAR, etc. Include copyright information.

13. SUPPLEMENTARY NOTES. Enter information not included elsewhere such as: prepared in cooperation with; translation of; report supersedes; old edition number, etc.

14. ABSTRACT. A brief (approximately 200 words) factual summary of the most significant information.

15. SUBJECT TERMS. Key words or phrases identifying major concepts in the report.

16. SECURITY CLASSIFICATION. Enter security classification in accordance with security classification regulations, e.g. U, C, S, etc. If this form contains classified information, stamp classification level on the top and bottom of this page.

17. LIMITATION OF ABSTRACT. This block must be completed to assign a distribution limitation to the abstract. Enter UU (Unclassified Unlimited) or SAR (Same as Report). An entry in this block is necessary if the abstract is to be limited.